nature water

Article

https://doi.org/10.1038/s44221-023-00131-3

Spatially separated crystallization for selective lithium extraction from saline water

In the format provided by the authors and unedited

This PDF file includes:

Supporting Notes:

Note S1

The selectivity between Li and Na is achieved by the solubility difference between LiCl and NaCl and the ion transport in the vertical and radial direction. For all different brine sources, NaCl and LiCl precipitates would only form when the ion activity product (IAP) exceeds the solubility product (K_{sp}). Therefore, since seawater has three orders of magnitude lower Li/Na wt. ratio to start with, the apparent selectivity improvement is more pronounced than the synthetic brine. This is advantageous compared with other DLE methods, which usually suffers from reduced selectivity when dealing with diluted lithium sources.

Note S2

The direct elemental characterization for Li has long been a challenge since Li has a low atomic number but is very active, so its radiation is very weak. Its characteristic X-rays are of too low energy (~55 eV) to be detected by Energy-dispersive X-ray spectroscopy (EDS), making conventional elemental analysis/imaging methods difficult to detect Li-salts. Therefore, researchers have tried indirect method to generate Li map, including using anion to indicate the lithium distribution[1,2]. To better prove the feasibility of this method for Li mapping, EDS mapping of a salt cluster consisting only NaCl and $MgCl_2$ were investigated. We found that the Mg mapping produced by deducting the Na map from the Cl map matches well with the experimental Mg mapping (**Fig. S16**). Therefore, when there are only NaCl and LiCl, as the case in the manuscript, a prediction of Li map could also be generated by deducting Na map from the Cl map. To further prove that the Na and Cl elements were only from the salt cluster not the crystallizer, we also scanned some pure NaCl crystal and the pristine crystallizer before experiment (**Fig. S17**). It showed that the original crystallizer material doesn't contain any NaCl, so the Na and Cl elemental signal should only be generated by the salt cluster collected within the crystallizer.

Note S3

The Péclet number (Pe) plays a crucial role in determining the relative significance of advection driven by evaporation and diffusion driven by concentration gradient, thereby impacting Li selectivity. Notably, the Péclet number for the fluid within the crystallizer at a temperature of 22°C and relative humidity of 22% was calculated to be 2647, representing the testing conditions depicted in **Fig. 1B** and **1C** and utilized for modeling shown in **Fig. 2H** and **2I**. Significantly reducing the Péclet number by a factor of 5 would lead to a 50% decrease in Li selectivity, which could be attributed to a substantially lowered

evaporation rate, increased salinity, or larger crystallizer porosity that offers less resistance to diffusion. Alternatively, increasing the evaporation rate by a factor of 5 could further improve Li selectivity. For instance, a 3 times higher evaporation rate was observed with an airflow of 1.5 m/s. Other strategies that could potentially enhance Li selectivity include reducing the porosity or radius of the crystallizer.

Note S4

This effect can be explained by introducing a model for the lifting height H, which results from a balance of capillary pressure (inducing an upward flow at the pore scale) and gravity (pulling the fluid downward). Typically, the lifting height produced by capillary forces can be modeled as $H = \gamma\sqrt{\phi}/(\rho g\sqrt{k})$, with γ the surface tension coefficient, g the acceleration of gravity and ϕ and k the medium porosity and permeability (respectively).

Supporting Figures

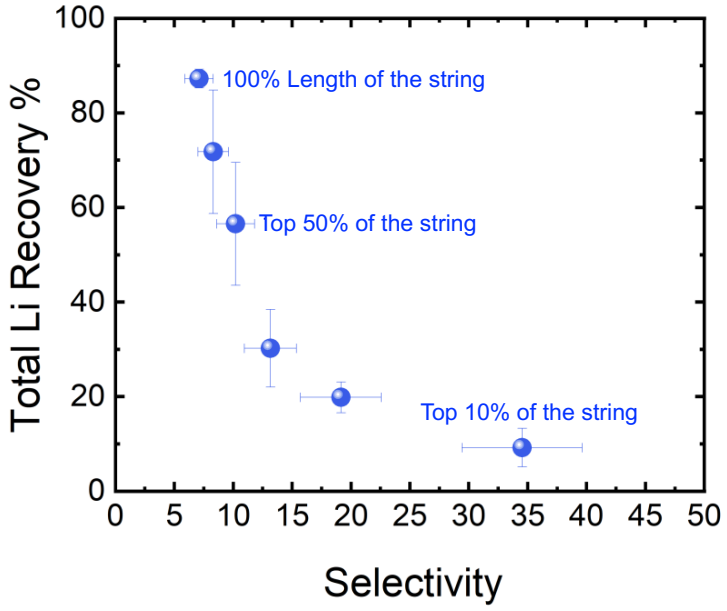

Figure S1. Li selectivity and recovery along the crystallizer. Error bars indicate the standard deviation of the total Li recovery and selectivity calculation from three independent samples (*n*=*3*). Data are presented as mean values ± standard deviation.

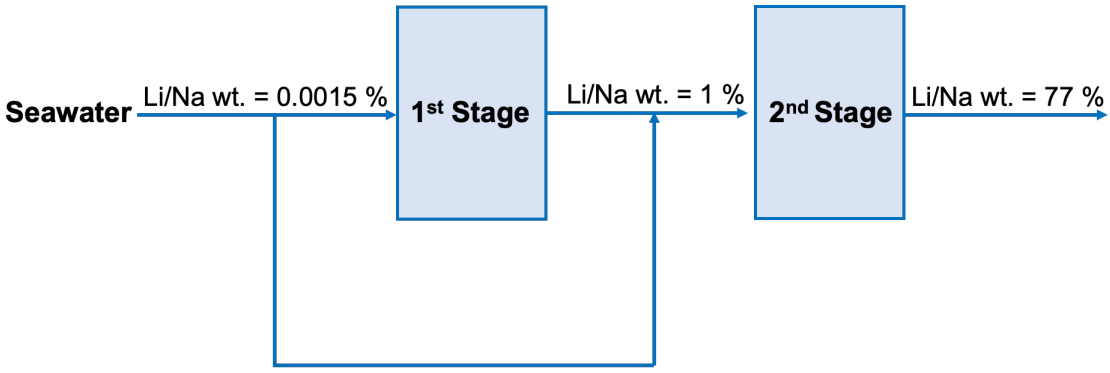

Figure S2. Schematic of multistage process for lithium purification from seawater.

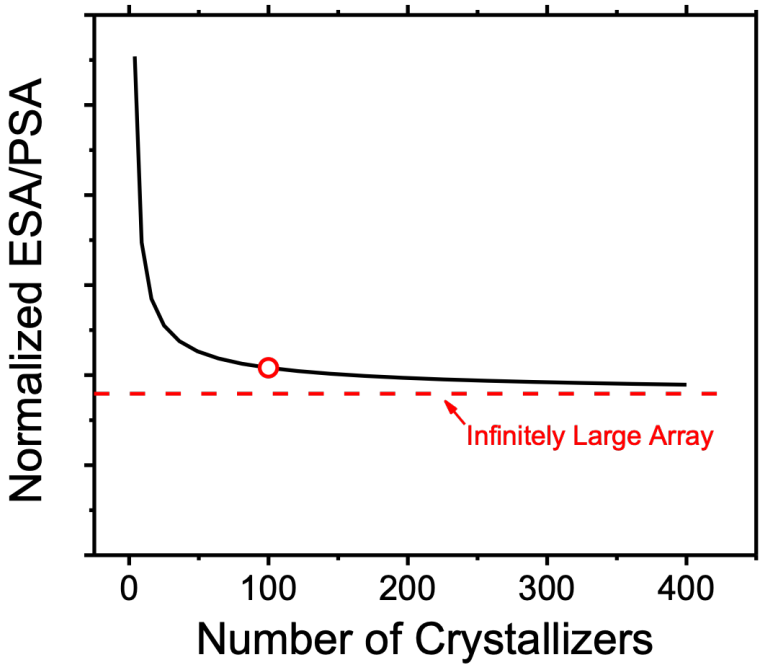

Figure S3. The normalized ESA/PSA ratio enlarged crystallizer numbers in an array. The magnitude of performance drop along with system scaling is closely related to the ratio between the evaporation surface area (ESA) and the projected surface area $(PSA)^3$. It exhibits the major performance change occurred in the beginning of array formation (< 50) and then approached to a plateau gradually.

Figure S4. The 4 strings are twisted tightly with an angle of 23~24° to the vertical.

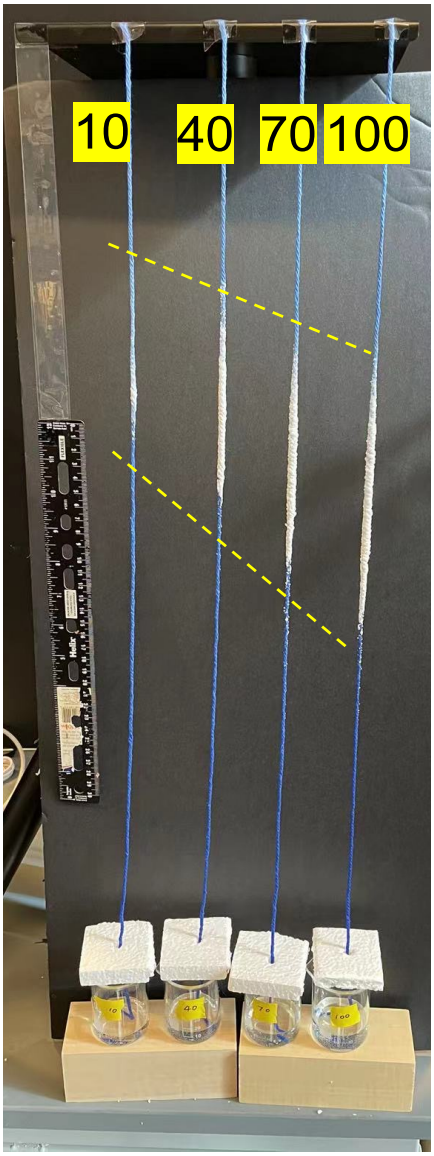

Figure S5. For saline waters containing different NaCl concentrations, salt crystallized at different heights on the crystallizer. From left to right, the saline water contains 10, 40, 70, and 100 g/L NaCl, respectively. Visible salt crystalized at different heights, with the lower concentration crystalized at a higher position.

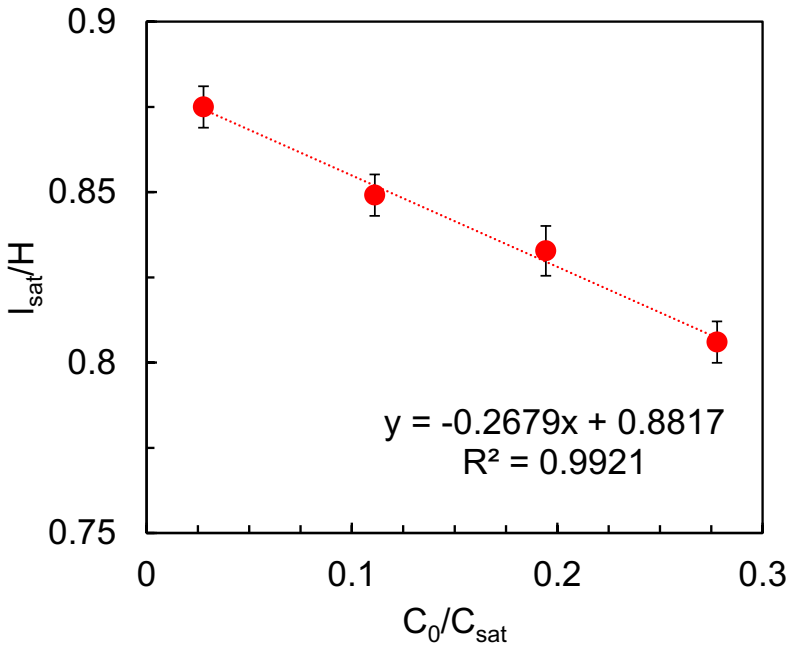

Figure S6. Concentration affects salt crystallization height. Error bars indicate the standard deviation of the crystallization height from triplicate experiments (*n*=*3*). Data are presented as mean values ± standard deviation.

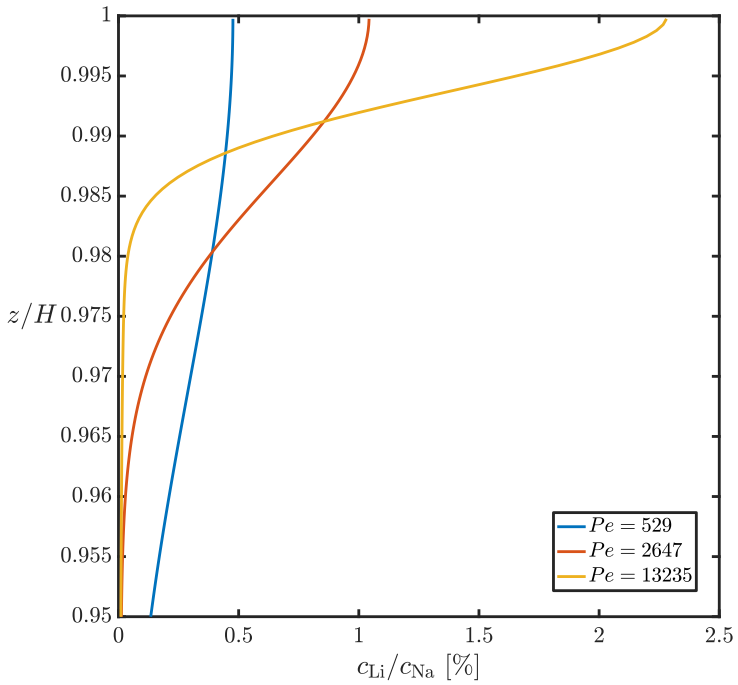

Figure S7. Effect of fluid mechanics inside of the crystallizer on Li selectivity

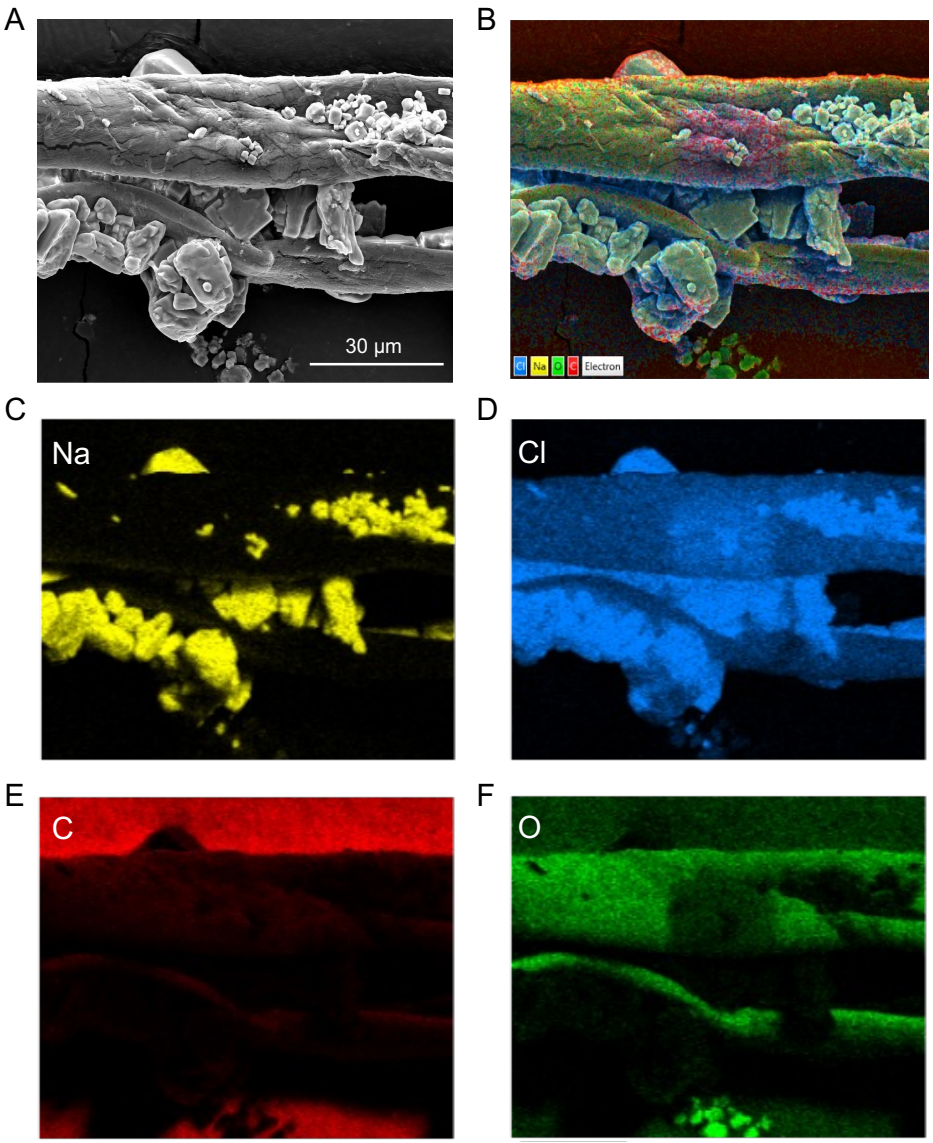

Figure S8. LiCl and NaCl distribution on fiber. The scanned fiber was separated from the top 5 cm of the crystallizer after Li extraction from brine water. (A) SEM image of the fiber. (B) Layered EDX map. (C-F) Na, Cl, C, and O map from the EDX. Only the cubic-shaped salt crystals emitted clear Na spectra, while the major fiber area showed no Na signal. Cl map shows a dispensed distribution over both the fiber and crystals. Cl needs a counterion to pair with, so the fiber area, with no Na signal but clear Cl signal, is hypothesized to be covered by Li.

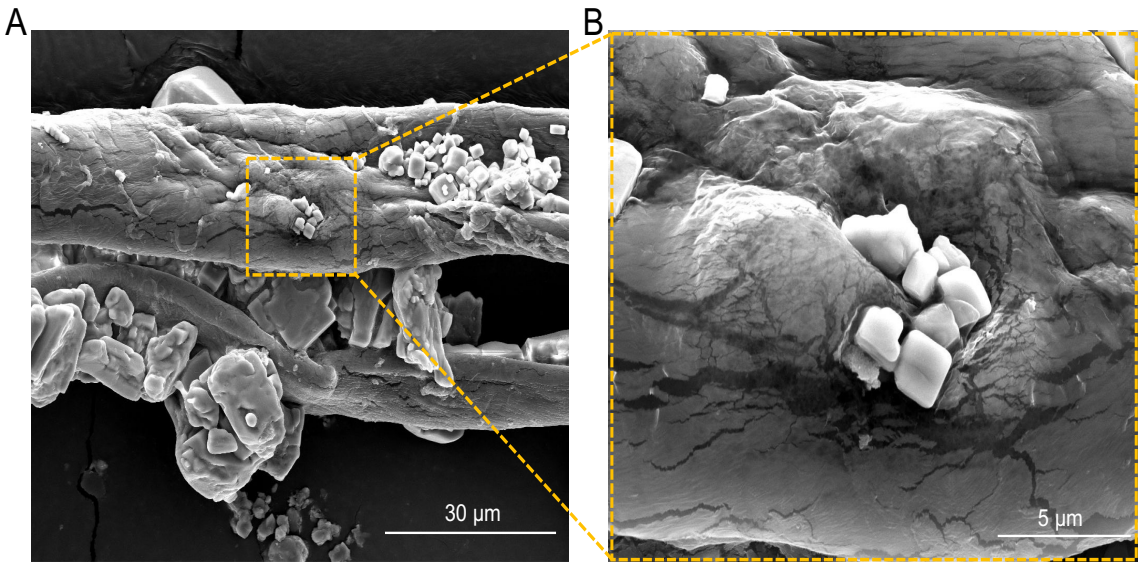

Figure S9. SEM image showing salt morphology on a fiber (A), zoom-in the yellow-boxed area for further investigation (B).

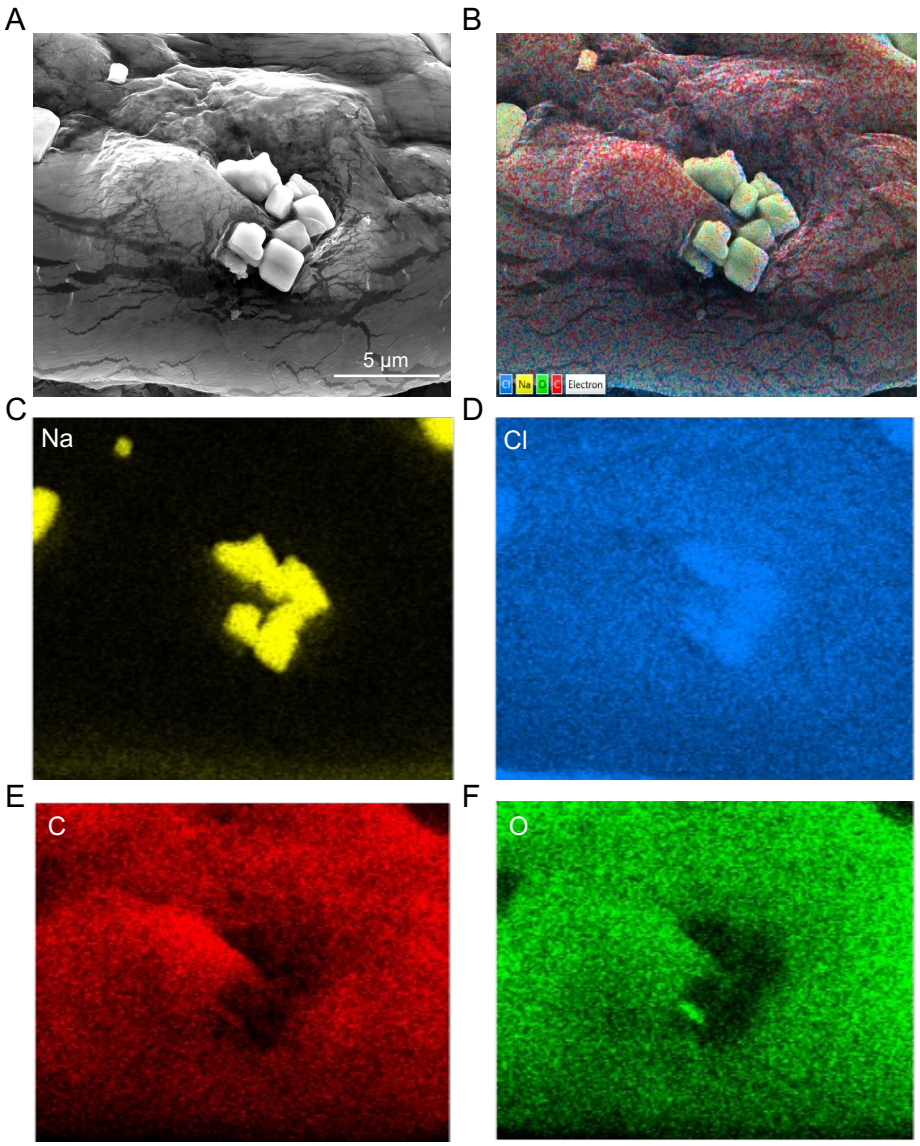

Figure S10. LiCl and NaCl distribution on fiber. (A) SEM image of the fiber. (B) Layered EDX map. (C-F) Na, Cl, C, and O map from the EDX. Only the cubic-shaped salt crystals emitted clear Na spectra, while the major fiber area showed no Na signal. Cl map shows a dispensed distribution over both the fiber and crystals. Cl needs a counterion to pair with, so the fiber area, with no Na signal but clear Cl signal, is hypothesized to be covered by Li.

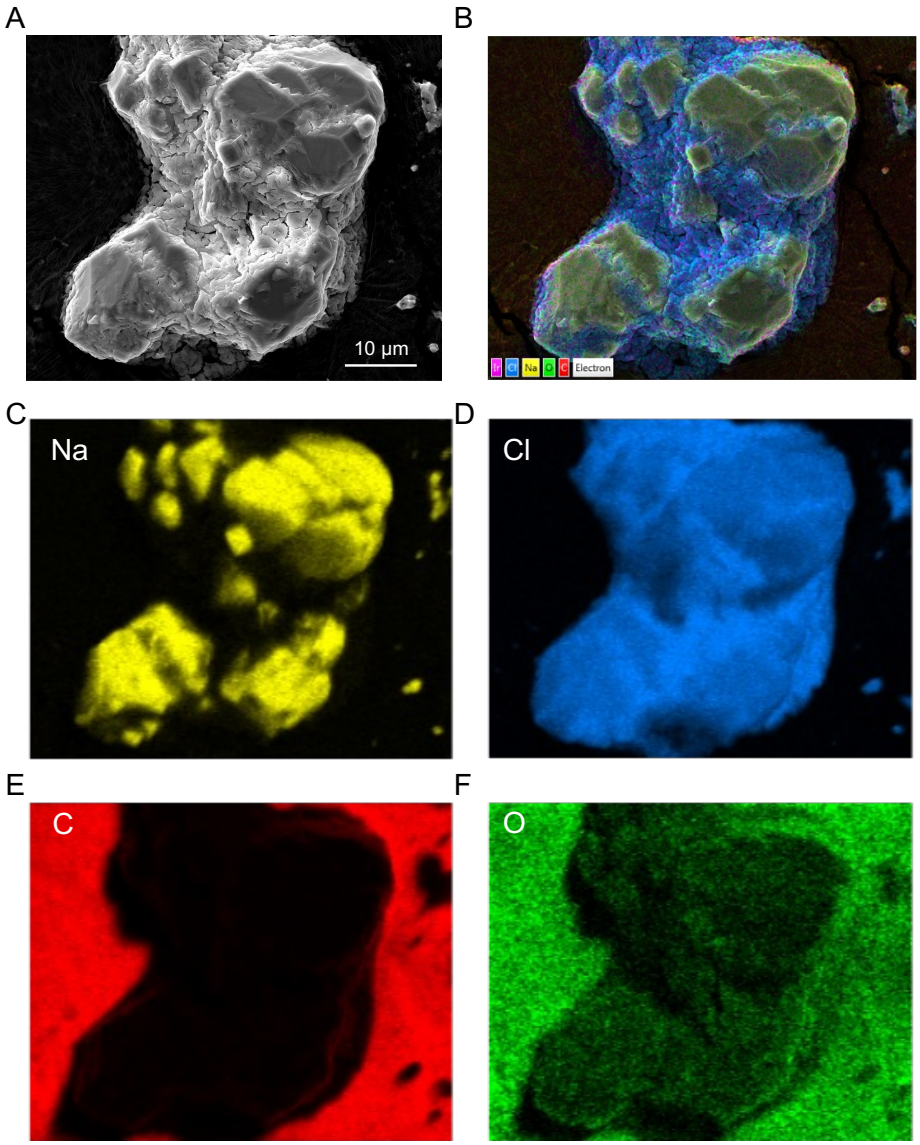

Figure S11. SEM-EDX characterization of the salt crystals collected from the top of the fiber crystallizer, Sample 1, salt crystal size ~ 50 µm. Salt crystals collected from the top 5 cm of the fiber crystallizer after Li extraction from brine water. (A) SEM image of the salt crystal. (B) Layered EDX map. (C-F) Na, Cl, C, and O map from the EDX. Only the big salt crystals emitted clear Na spectra, while the salt filled in between the big salt crystals showed no Na signal (C). In contrast, Cl map covered the whole crystal (D). Since Cl needs a counterion to pair with, the salt filled in between the big salt crystals, with no Na signal but clear Cl signal, is hypothesized to contain Li.

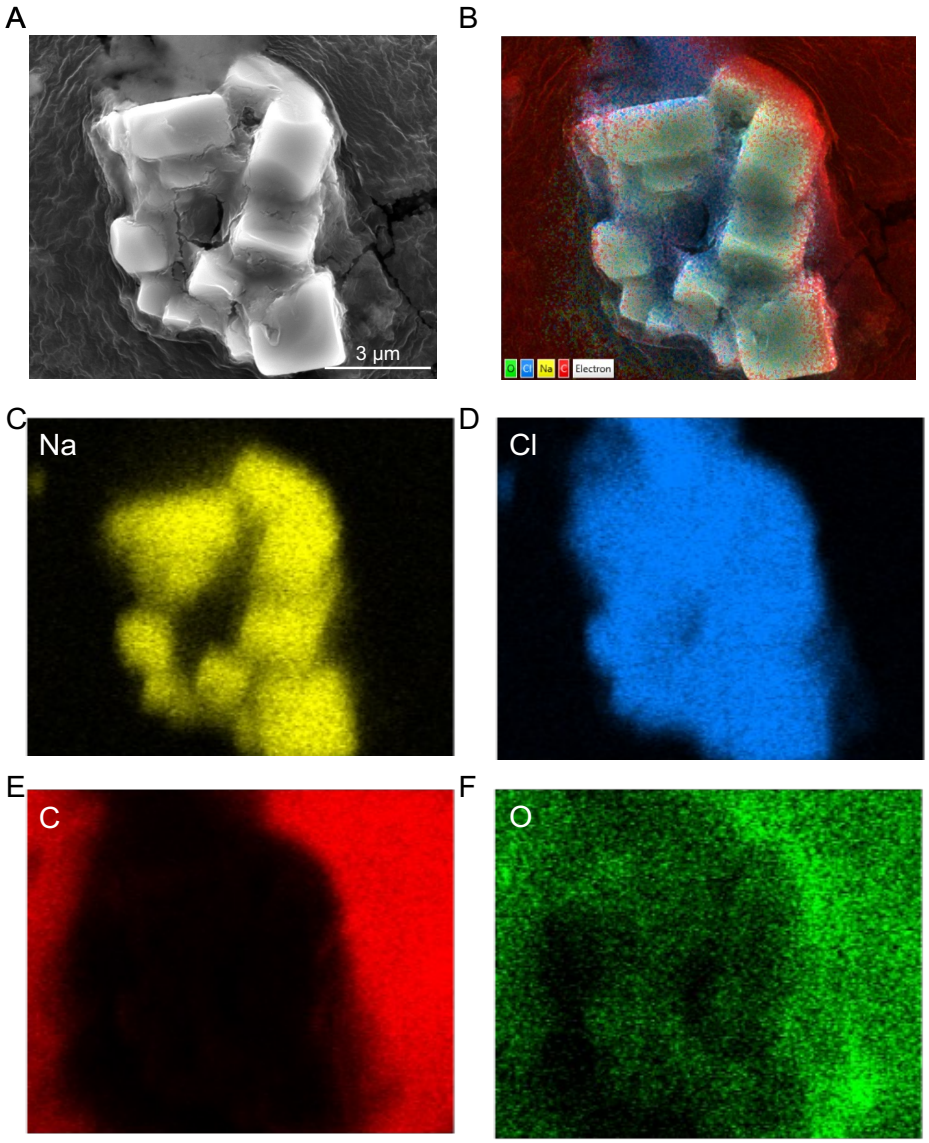

Figure S12. SEM-EDX characterization of the salt crystals collected from the top of the fiber crystallizer, Sample 2, salt crystal size ~ 5 µm. Salt crystals collected from the top 5 cm of the fiber crystallizer after Li extraction from brine water. (A) SEM image of the salt crystal. (B) Layered EDX map. (C-F) Na, Cl, C, and O map from the EDX. Only the big salt crystals emitted clear Na spectra, while the salt filled in between the big salt crystals showed no Na signal (C). In contrast, Cl map covered the whole crystal (D). Since Cl needs a counterion to pair with, the salt filled in between the big salt crystals, with no Na signal but clear Cl signal, is hypothesized to contain Li.

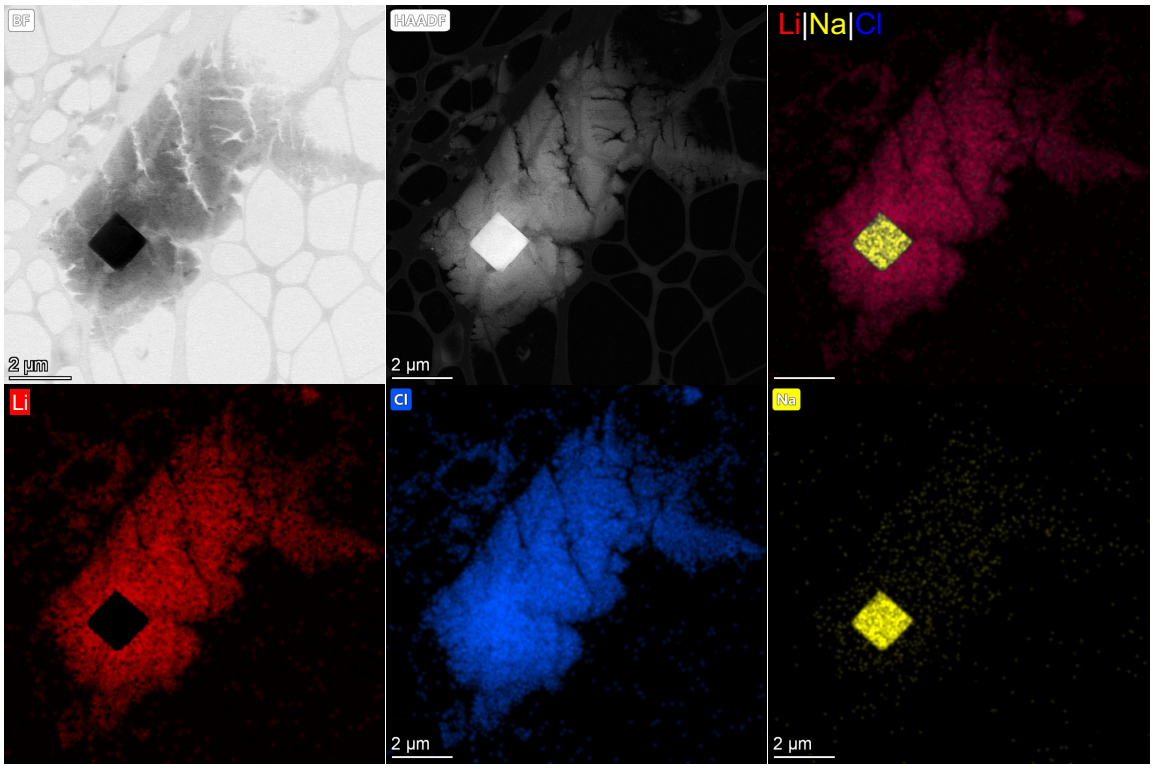

Figure S13. STEM-EDX images showing LiCl surrounds NaCl, sample No.2. Li map was achieved by filter Cl map by Na map.

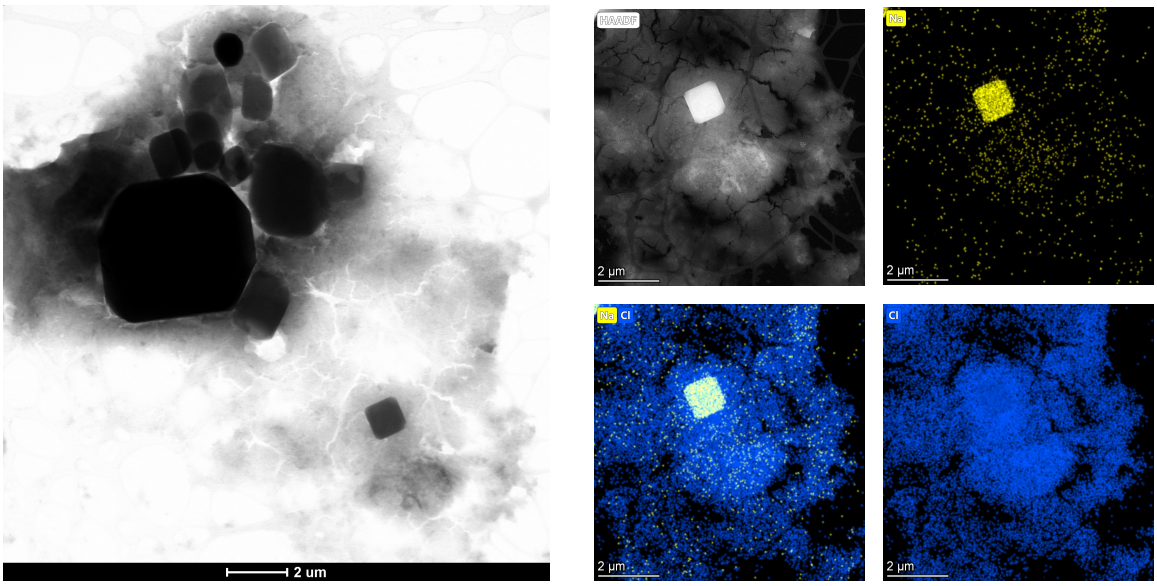

Figure S14. STEM-EDX images showing LiCl surrounds NaCl, Sample No.3.

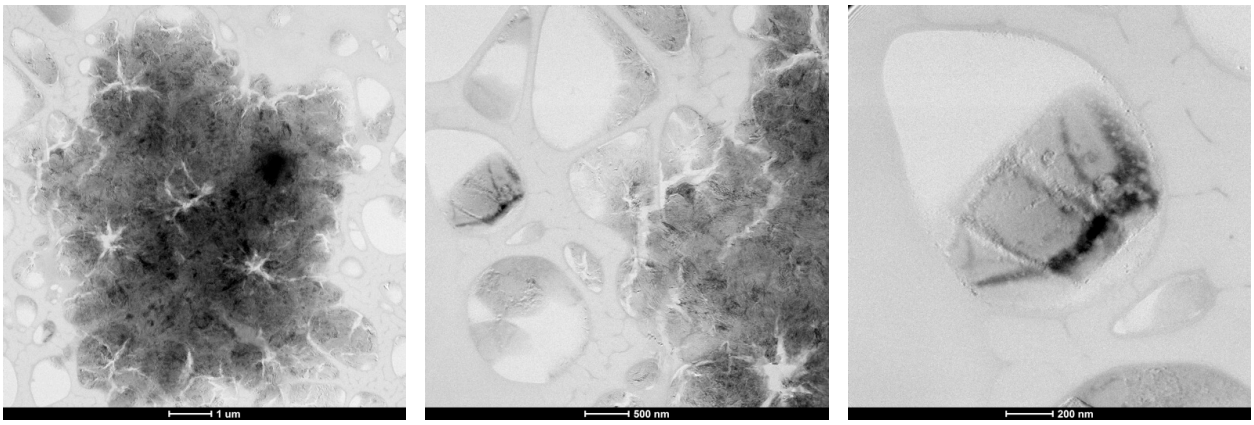

Figure S15. STEM image showing the thin layer salt. Based on the previous investigation, this shape should be LiCl salt, indicating an easy separation of LiCl and NaCl crystals.

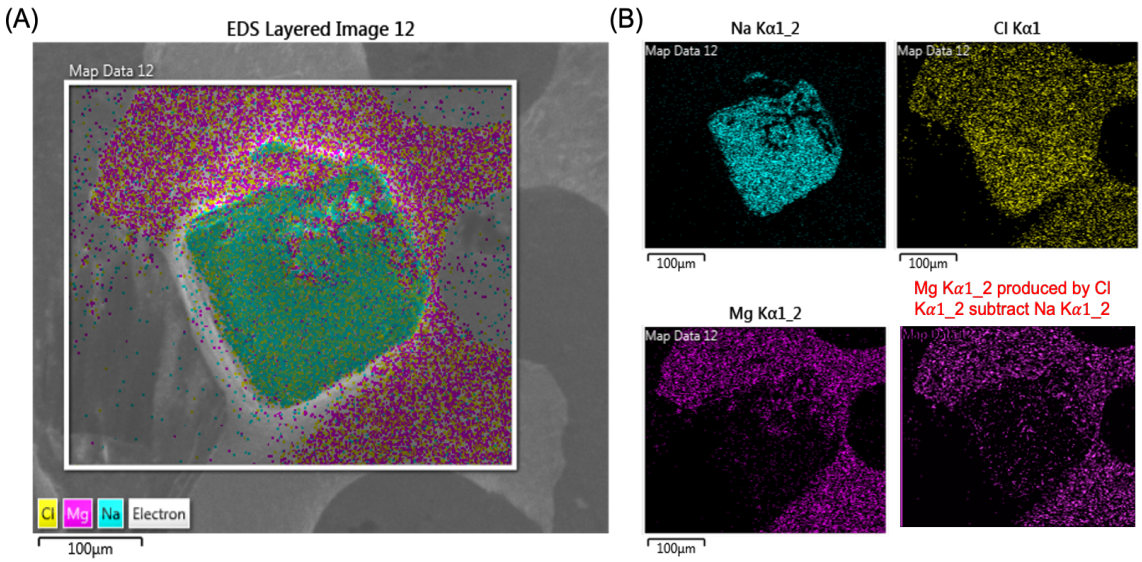

Figure S16. Indirect method for element mapping. (A) EDS scanning results for a salt cluster containing only NaCl and $MgCl_2$. (B) EDS elemental scanning results for Na, Cl, Mg, and the indirect Mg map generated by deducting Na map from Cl map.

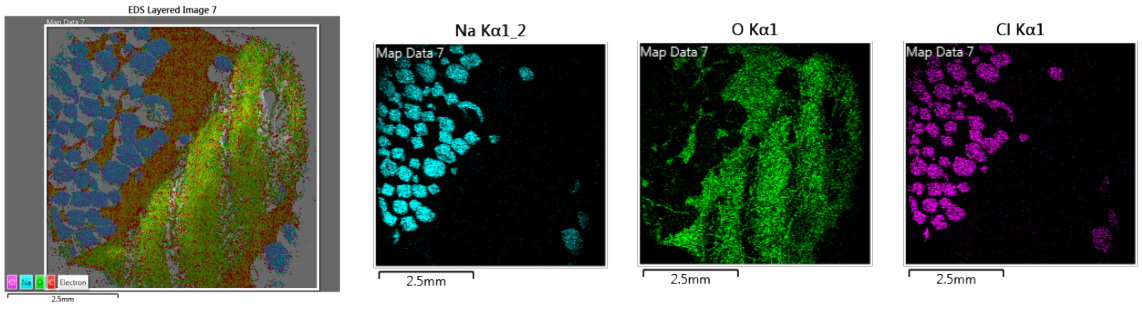

Figure S17. EDS element mapping of original string (right) with NaCl crystals as reference (left), where Cl was not detected on the original string.

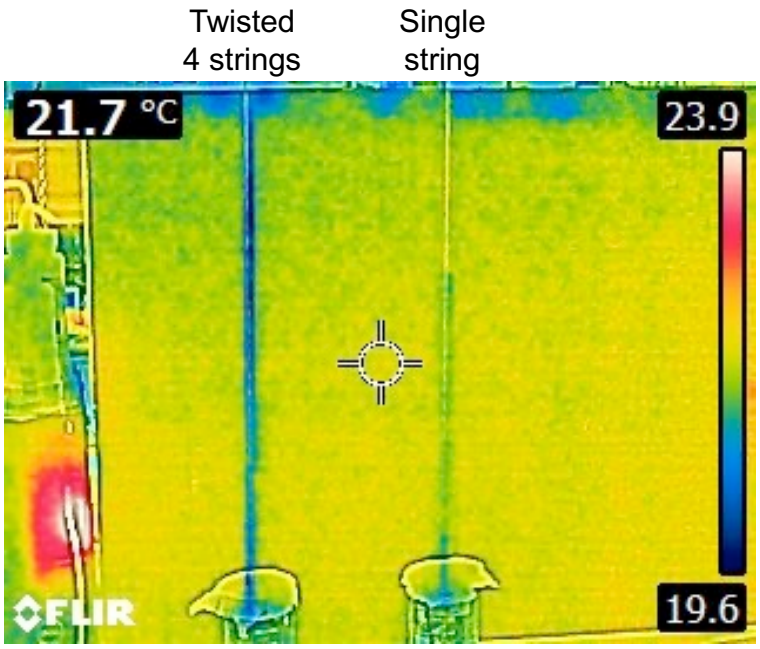

Figure S18. Twisting more fiber strings into the crystallizer can improve water lifting. FLIR image showing the twisted 4 stings can lift water higher than the single sting. Model for the lifting height $H = \gamma\sqrt{\phi}/(\rho g\sqrt{k})$ provides an explanation for this effect: as the packing of fibers and strings increases with twisting, the effective pore size of the evaporator decreases, thereby reducing its permeability k and increasing H.

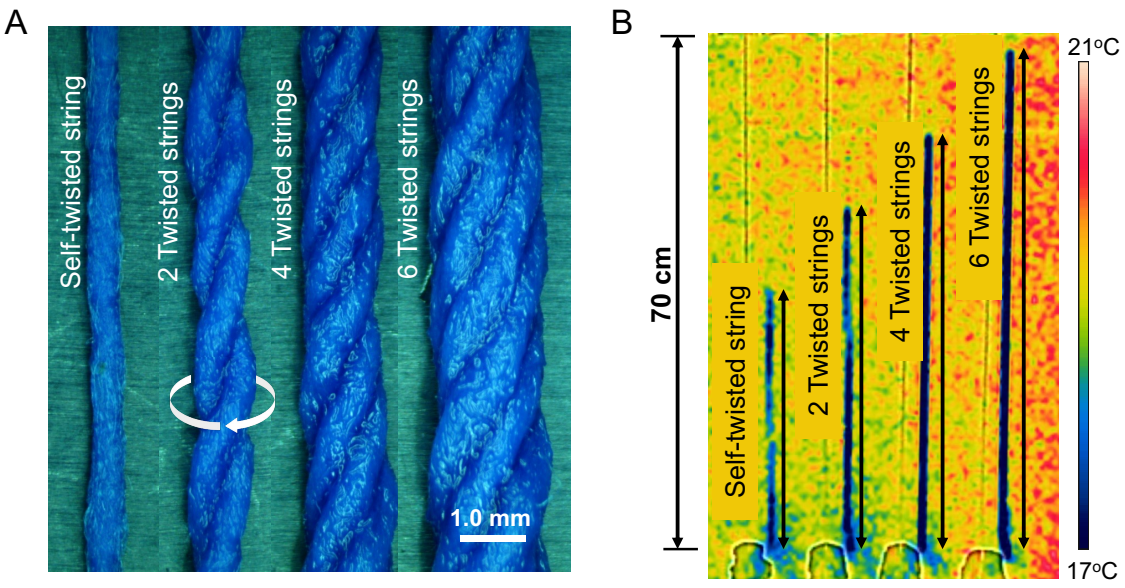

Figure S19. (A) Optical image of the self-twisted string, 2, 4, and 6 twisted strings. (B) FLIR image showing the 4 twisted stings can lift water higher than the self-twisted sting. Twisting every 2 more strands in the textile structure can lift water by ~10-15% higher.

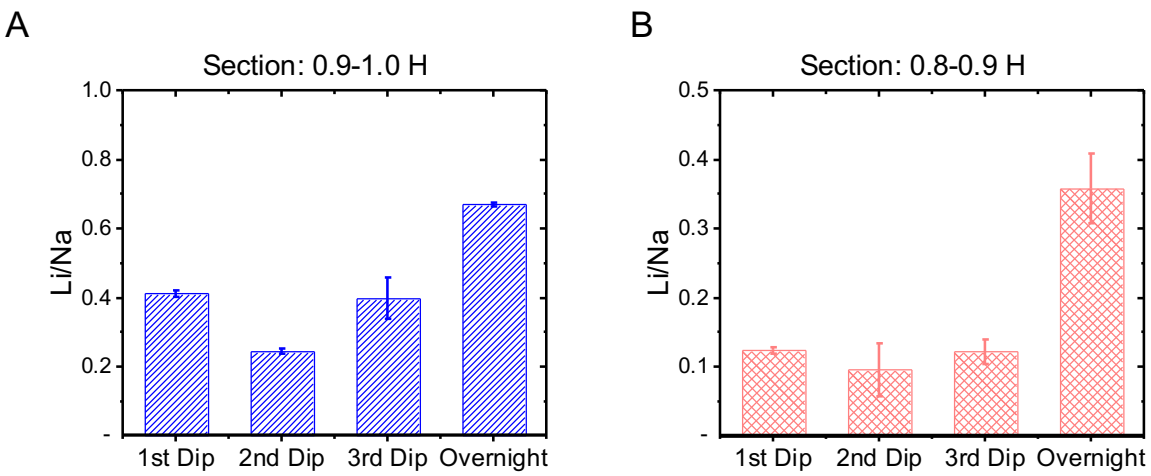

Method:
Dip the yarn into the 1st 10 mL DI water for 1s;
Dip the yarn into the 2nd 10 mL DI water for 1s;
Dip the yarn into the 3rd 10 mL DI water for 1s;
Soak the yarn in 10 mL DI water and let salt fully dissolve overnight.

Figure S20. Wash-soak can facilitate LiCl recovery. For the top 0-5 cm (A) and 5-10 cm (B) crystallizer, both the final Li/Na ratios can be further increased by repeating the wash-soak method. Error bars indicate the standard deviation of the Li/Na from triplicate experiments (*n*=*3*). Data are presented as mean values ± standard deviation.

Supporting Movie Legends

Movie S1. Easy peeling of the Na-rich salt shell for Na separation, sampled after 5 days' spatial crystallization for Li extraction from seawater.

Movie S2. 3D structure of the 4-strings-twisted fiber crystallizer. Movie constructed by AVIZO software upon 3D X-ray scanning images.

Movie S3. Time lapse video records the growth of the crystals during the operation. From left to right, the saline water contains 10, 40, 70, and 100 g/L NaCl, respectively. Visible salt crystalized at different heights, with the lower concentration crystalized at a higher position.

References

1. Li, C. *et al.* Mapping Techniques for the Design of Lithium-Sulfur Batteries. *Small* **18**, 1–14 (2022).
2. Adhitama, E. *et al.* Pre-Lithiation of Silicon Anodes by Thermal Evaporation of Lithium for Boosting the Energy Density of Lithium Ion Cells. *Adv. Funct. Mater.* **32**, (2022).
3. Zheng, S. *et al.* Upscaling 3D Engineered Trees for Off-Grid Desalination. *Environ. Sci. Technol.* **56**, 1289–1299 (2022).